Spectral Band Selection from *casi* Data for Monitoring Mine Tailings Site Rehabilitation

Josée Lévesque
MIR Télédétection Inc., 2182 de la Province, Longueuil, QC, J4G 1R7, Canada
Email : levesque@ccrs.nrcan.gc.ca

Tom Szeredi
MacDonald Dettwiler and Assoc., 13800 Commerce Parkway, Richmond, BC, V6V 2J3, Canada

Karl Staenz, Vern Singhroy
Canada Centre for Remote Sensing, 588 Booth St., Ottawa, ON, K1A 0Y7, Canada

***Abstract* – This paper investigates the effect of varying bandwidth and number of bands on spectral unmixing results of *casi* data acquired over a mine tailings site. Forthcoming high spatial resolution sensors with less bands and larger bandwidths such as Quickbird, Ikonos1 and Orbview3 were simulated in order to determine whether the similar unmixing results can be achieved as with the 68-band *casi* data.**

1. INTRODUCTION

Canadian liability for acid mine drainage is in the order of $2 billion to $5 billion depending on the technique used to dispose of and treat the acidic waste (MEND). In the Sudbury area alone, Inco Ltd. spends an annual $5 million to reclaim property (Inco Ltd.). Given these enormous costs, monitoring techniques are needed to evaluate the efficiency of the techniques used to revegetate mine tailings sites. In a previous study, Lévesque et al. (1997) demonstrated the monitoring capability of the Compact Airborne Spectrographic Imager (*casi*) over the Sudbury mine tailings area. If long term monitoring is required airborne surveys can become quite expensive. The question is whether one can achieve similar results using forthcoming high spatial resolution satellites such as Quickbird, Ikonos1, and Orbview3 (Table 1). The spatial resolution of these sensors is similar to that of the *casi* data acquired over the Sudbury mine tailings site (2.3 m by 4.3 m). However, these sensors have fewer spectral bands and their bands are wider than those of the *casi* dataset used in this study. This paper investigates the effect of varying bandwidth and number of bands on spectral unmixing results. Finally, four Quickbird bands and related bandwidths were simulated in order to evaluate their possible monitoring capability. Since Orbview3 and Ikonos1 have basically the same spectral configuration as Quickbird the results obtained for Quickbird are assumed to be applicable to these sensors also.

Table 1. Spectral band configuration and spatial resolution for the Quickbird, Orbview3 and Ikonos sensors.

Sensor	Quickbird	Orbview3	Ikonos1
Company	Earthwatch	Orbital Sciences	Space Imaging
Spectral bands (nm)	450 - 520 530 - 590 630 - 690 770 - 900	450 - 520 520 - 600 625 - 695 760 - 900	450 - 520 520 - 600 630 - 690 760 - 900
Spatial resolution	3.2 m	4 m	4 m

2. METHODOLOGY

2.1 Image data

Hyperspectral *casi* radiance data were acquired on August 24, 1996 in 72 contiguous, 8.7 nm wide, spectral bands covering a wavelength range from 407 nm to 944 nm. Pixel size is 2.3 m in the across track direction and 4.3 m in the along track direction. Table 2 summarizes the *casi* sensor configuration parameters. Only wavelengths between 407 nm and 900 nm (68 bands) were used due to the poor spectral quality of the last four bands.

Table 2. *casi* sensor configuration.

Spectral coverage	407-944 nm
Number of bands	72
Spectral sampling interval	7.6 nm
Bandwidth at FWHM*	8.7 nm
Sensor altitude above ground	1905 m
Ground resolution: across track	2.3 m
along track	4.3 m
Swath	406 pixels

* FWHM: Full Width at Half Maximum

2.2 Image data preprocessing

The *casi* image data were roll corrected using the navigation data to remove most significant aircraft motion effects from the imagery. Surface reflectance was retrieved from the radiance data using a look-up table based approach implemented in the Imaging Spectrometer Data Analysis System (ISDAS) (Staenz et al., 1997 and 1998).

2.3 Band simulation

Band reduction. The number of bands were reduced by skipping every other band of the 68-band *casi* dataset resulting in a 34-band dataset. This procedure was repeated to produce datasets containing 17, 8, and 4 bands, respectively.

Varying bandwidth. In order to test the effect of varying the bandwidth on the unmixing results, 6 bands were chosen based on the geobotany dataset from Staenz (1996) (480 nm, 548 nm, 608 nm, 676 nm, 745 nm, 829 nm). A gaussian spectral response profile centered at each of the 6 selected bands was used to simulate the bandwidths ranging from 8.5 nm to 76.5 nm with an increment of 8.5 nm.

Sensor simulation. Quickbird spectral bands as shown in Table 1 were simulated using gaussian spectral response profiles.

2.4 Spectral unmixing

Constrained spectral unmixing was performed on all the simulated *casi* data cubes using an algorithm implemented in ISDAS (Szeredi et al., 1998 ; Boardman, 1989 and 1990). The method decomposes the image spectra $\vec{S}$ in terms of endmember spectra $\vec{S}_i$:

$$\vec{S} \approx \sum_{i=1}^{N} f_i \vec{S}_i \qquad \textbf{(1)}$$

where $0 \le f_i \le 1$, $\sum_{i=1}^{N} f_i = 1$ and f_i is the fraction of endmember *i* contributing to the image spectrum $\vec{S}$, and N is the total number of endmembers. The result of the unmixing is a set of N fraction images which show the fractional abundance of the endmembers. Endmember spectra were selected from the original image using the three first principal components (PCs) which account for 77%, 21% and 1% of the variability in the dataset, respectively. Endmembers are the purest pixel spectra in the dataset and are often located at the extremities of the scatterplot when two PCs are plotted against each other. Five endmember spectra were identified as shown in Figure 1: lime, green vegetation, oxidized tailings, water 1, and water 2 (distinct from water 1 because of it's high content of sewage, tailings, and lime). According to the PC scatterplots, the endmember spectra were the same for the band reduced, varying bandwidth, and sensor simulation data cubes. The unmixing results of the simulated datasets were then compared to the unmixing results of the full 68-band dataset. Comparison between the 68-band dataset unmixing results and the unmixing results from the simulated cubes was achieved by computing the absolute and relative difference.

3. RESULTS

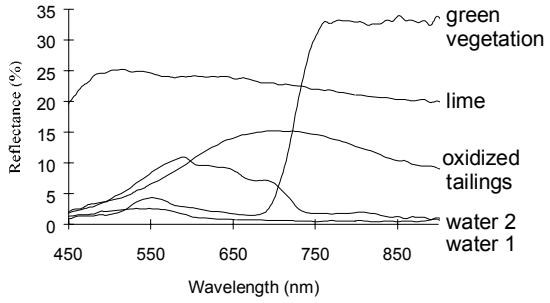

Figure 1. Endmember spectra.

The relative difference between the Quickbird simulation and the 68-band unmixing results is shown in Figure 2 for the green vegetation endmember. The plot shows that low fractions display a larger relative difference than higher fractions. For a constant absolute difference this result is to be expected.

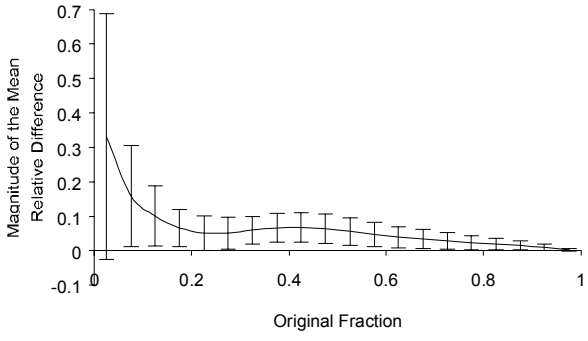

Figure 2. Relative difference (solid curve) and standard deviation (vertical bars) for the green vegetation endmember between unmixing results achieved with Quickbird simulated data and the 68-band *casi* data.

3.1 Band reduction

Figure 3 shows the effect of varying the number of *casi* bands on the spectral unmixing results. The absolute mean difference (AMD) remains under 0.02 for all the endmembers using 34, 17, and 8 bands. When using 4 bands the overall AMD increases but remains below 0.03 for green vegetation and lime. The two water endmembers consistently display a higher AMD than the other endmembers. This can be understood from eq. (1). The water endmember spectra $\vec{S}_{w1}$, $\vec{S}_{w2}$, are relatively dark, hence the spectral magnitudes $|\vec{S}_{w1}|$ and $|\vec{S}_{w2}|$ are small compared to the other endmembers. Due to this fact the fractions f_{w1} and f_{w2} can vary by a relatively large amount without changing the sum spectrum in eq.(1) too much. The constrained unmixing takes advantage of this fact and hence the fractions f_{w1} and f_{w2} vary more than the fractions of the other endmembers.

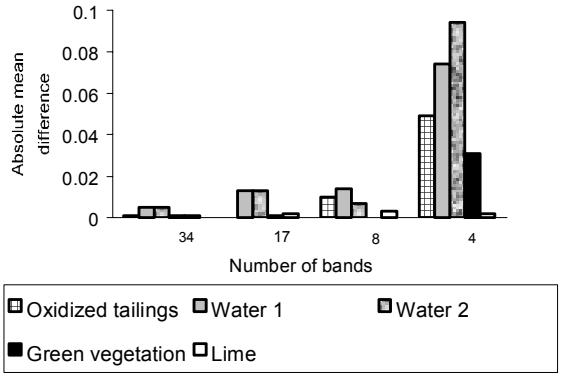

Figure 3. Absolute mean difference (AMD) between the 68-band unmixing results and unmixing results of a varying number of bands for each endmembers.

3.2 Varying bandwidth

Figure 4 shows the AMD and its standard deviation between the 68-band unmixing results and the varying bandwidth of the 6 selected band data cube. AMD slightly increases with increasing bandwidth but the AMD remains below 0.005. The standard deviation of the AMD decreases as the bandwidth increases since the local variations (in wavelength) in the spectrum are smoothed over. This results in less fractional variations and a smaller standard deviation.

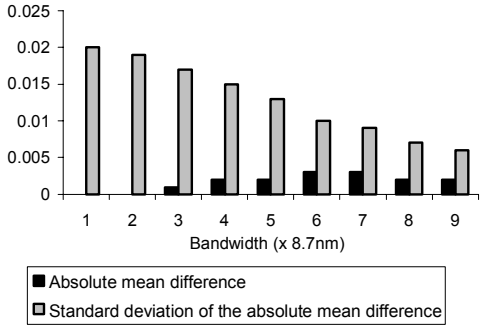

Figure 4. Absolute mean difference (AMD) and standard deviation between the 68-band umixing results and the unmixing results of varying bandwidth of the 6-band datacube.

3.3 Sensor simulation

In Figure 5 the AMD is shown for each endmember for the Quickbird simulation unmixing results against the 68-band unmixing results. Unlike for the case of four bands used in Figure 3, the four Quickbird bands were selected to enhance differences between the spectra and hence display lower AMD. As pointed out before, the two water endmembers, followed by the oxidized tailings, the green vegetation and the lime endmembers, show an inverse relationship between their spectral reflectance magnitude and their AMD. AMD values for all endmembers do not exceed 0.015. Similarly, the standard deviation of the AMD is related to the magnitude of the endmember spectra which indicates that more variation is expected when using low reflectance endmembers.

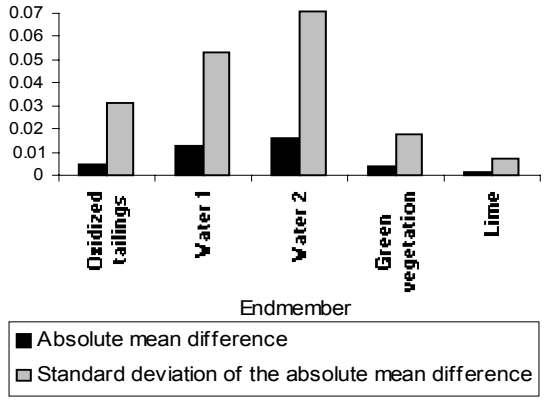

Figure 5. Absolute mean difference (AMD) between the 68-band unmixing results and the Quickbird simulation unmixing results for each endmember.

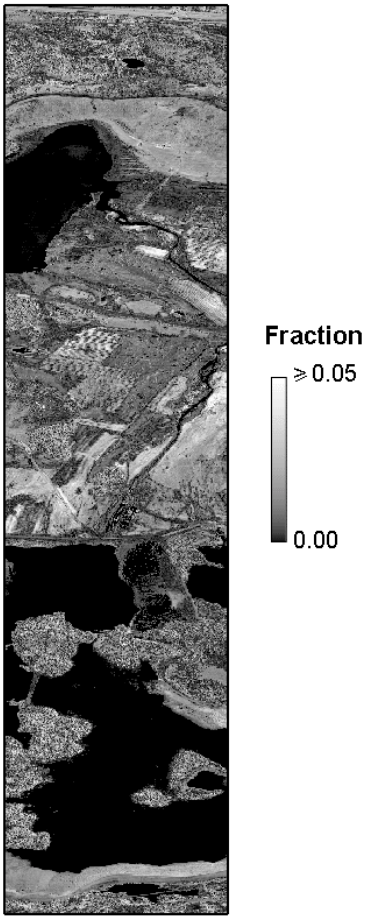

Figure 6. Map of the absolute difference (AD) between Quickbird simulation unmixing results and the 68-band unmixing results over the Copper Cliff mine tailings area in Sudbury.

The map shown in Figure 6 gives a spatial representation of the absolute difference (AD) between the Quickbird simulation unmixing results and the 68-band unmixing results over the Copper Cliff mine tailings area in Sudbury. The brighter parts of the map show higher differences and the darker parts show lower differences. Most of the data are in the AD range of 0.00 to 0.05.

4. CONCLUSION AND DISCUSSION

The unmixing results obtained by varying the number of bands produce absolute mean differences that do not exceed 0.02 for 34-band, 17-band and 8-band sets. The 4-band dataset yields larger differences, up to 0.094. However, Quickbird simulation indicates a difference of 0.016 is achievable if the bands are selected according to physical spectral properties. The bandwidth simulation results indicate that as bandwidth increases, the absolute mean difference increases and the standard deviation of the absolute mean difference decreases. The study shows that similar unmixing results are obtained using *casi* hyperspectral data and simulated broad-band high resolution multispectral sensors.

However, several points must be borne in mind: the limited spectral resolution of broad-band sensors make it difficult to spectrally identify endmembers and to spectrally separate subtle differences in endmembers. The endmembers in this study are very spectrally different and hence the second point was not a problem. To unmix a scene with N endmembers requires N-1 bands. Therefore, complicated scenes with many endmembers might require more bands to perform spectral unmixing than provided by forthcoming high spatial resolution sensors.

5. REFERENCES

Boardman, J.W., "Inversion of Imaging Spectrometry Data Using Singular Value Decomposition", *Proceedings of the 1989 International Geoscience and Remote Sensing Symposium (IGARSS '89) and the 12th Canadian Symposium on Remote Sensing*, Vancouver, BC, Vol. 4, pp. 2069-2072, 1989.

Boardman, J.W., "Inversion of High Spectral Resolution Data", *Proceedings of SPIE Conference on Imaging Spectrometry of the Terrestrial Environment*, Orlando, Florida, Vol. 1298, pp. 222-233, 1990.

Lévesque, J., Szeredi, T., Staenz, K., Singhroy, V., and Bolton, D., "Spectral Unmixing for Monitoring Mine Tailings Site Rehabilitation, Copper Cliff Mine, Sudbury, Ontario", *Proceedings of the Twelfth International Conference and Workshops on Applied Geological Remote Sensing*, Denver, Colorado, Vol. 1, pp.340-347, 17-19 November 1997.

Mend - Mine Environmental Neutral Drainage program: http://www.nrcan.gc.ca/mets/mend, 1998.

Inco Ltd : http://www.incoltd.com/invest/annrpt/96-env1g.htm, 1998.

Staenz, K., "Classification of a Hyperspectral Agricultural Data Set using Band Moments for Reduction of the Spectral Dimensionality", *Canadian Journal of Remote Sensing*, Vol. 22, No. 3, pp. 248-257, 1996.

Staenz, K., and Williams D., "Retrieval of Surface Reflectance From Hyperspectral Data Using a Look-Up Table Approach", *Canadian Journal of Remote Sensing*, Vol. 23, No. 4 , pp. 354-368, 1997.

Staenz, K., Neville, R.A., Lévesque, J., Szeredi, T., Singhroy, V., Borstad, G.A., and Hauff, P., "Evaluation of *casi* and SFSI Hyperspectral Data for Geological Applications - Two Case Studies", *in Geological Remote Sensing/ Case Studies* (editor V. Singhroy), Geological Association of Canada (GAC) Special Paper (in press), 1998.

Szeredi, T., Staenz, K., and Neville, R.A., "Spectral Unmixing in ISDAS", to be submitted to: *Canadian Journal of Remote Sensing*, 1998.